Communication

Null Steering in Linear Array Antennas With Electronically Displaced Phase Center Dual-Mode Antenna Elements

Tanzeela Mitha and Maria Pour

***Abstract*— The potential of dynamically steering the null locations in equally spaced linear scanning array antennas using the electronically displaced phase center antenna (E-DPCA) technique is investigated for the first time in this communication. The relative coordinates, and thus, the element spacing, of the equally spaced linear array antennas are electronically varied using the E-DPCA technique to adaptively steer the null locations without any physical displacement while maintaining the same overall array length. The versatility of the proposed technique is further explored by: 1) generating consecutive nulls with a minimum resolution of 1° between them and 2) simultaneously steering the null locations and scanning the main beam.**

***Index Terms*— Beam scanning, electronically displaced phase center antenna (E-DPCA), null steering phased array antennas.**

I. Introduction

Classical array pattern synthesis techniques focus on reducing the sidelobe level (SLL) and controlling the null locations to reduce unwanted interference and prevent jamming. Array pattern null locations can be steered in the direction of the interfering signal by controlling the excitation coefficients of the antenna element, namely phase-only, amplitude-only, and both the phase- and amplitude-control techniques [1], [2], [3], [4], [5], [6], [7], [8], [9], [10], [11]. A major drawback of engaging the phase shifters in the null steering application is its restriction on the scanning capability of the main beam toward the desired direction. An alternate method of controlling the null location is the element position perturbation technique [12], [13], [14]. Different optimization algorithms have been developed to determine the ideal amplitude/phase-excitation as well as the optimal positions of physically aperiodic array elements to steer the nulls toward jammers [15], [16], [17], [18], [19], [20], [21]. As the direction of the interfering signal can dynamically vary, the elements of the array need to be constantly moved to different locations. For physically aperiodic arrays, this may be achieved by attaching servomotors to each element. However, as the array size increases, the overall cost and complexity of the position-control mechanism grow, making the system difficult to implement. To mitigate this, a new method of adaptive null steering using the electronically displaced phase center antenna (E-DPCA) technique, without any mechanical means, is proposed for the first time in this communication.

The DPCA technique [22] has been used in a single-aperture antenna [23], [24], [25], as well as in multimode patch antennas [26], [27], [28], to create virtual arrays without having to physically move the antennas. Recently, Mitha and Pour [29], [30] utilized the E-DPCA technique in small two- and three-element arrays as well as larger N-element linear array antennas to vary the overall aperture size and reduce the SLL and minor lobe level, respectively. Herein, the E-DPCA technique is initially employed in a nine-element linear array to adaptively steer symmetric null locations without physically moving its constitutive elements. The versatility of the E-DPCA technique is further explored in a 25-element equally spaced linear array where: 1) two consecutive nulls are generated with a minimum resolution of 1° between them; 2) the side and minor lobes are reduced by 5 dB while steering the null location; and 3) simultaneous null steering and beam scanning are realized without any physical displacement.

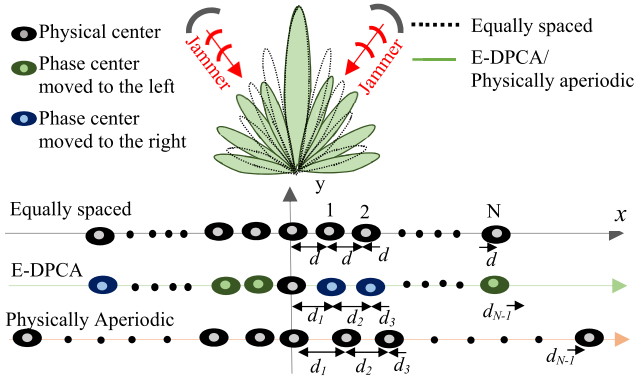

Fig. 1. Illustrative comparison of the physically aperiodic and E-DPCA array configurations that steer the nulls toward the direction of jammers. The length of the E-DPCA array is the same as its equally spaced counterpart, without any physical displacement.

An illustrative comparison of the typical configurations of the equally spaced array with the physically aperiodic and the proposed E-DPCA arrays is drawn in Fig. 1, wherein, the E-DPCA array maintains the same array length while dynamically steering the null location toward the jammers, without any mechanical means. It is worth noting that the technique may be applied to any antenna element with the electronically displaced phase center capability, such as multimode microstrip patches and open-ended waveguides.

II. Null Steering Using the E-DPCA-Based Position Control Technique

The total E_θ radiation pattern of a $(2N+1)$-element, equally spaced E-DPCA array with the x-polarized TM_{11} and TM_{21} modes of circular microstrip patches is given by [26], [27], [28], [29], [30]

$$E_\theta^{Total} = \sum_{n=-N}^{N} a_p(n)\, E_\theta(n)\, e^{j[k_0 nd \sin\theta cos\phi + \beta(n)]} \tag{1}$$

where

$$E_\theta(n) = -\frac{je^{-jk_0 r}}{r}\left\{\left[J_0(u_1) - J_2(u_1)\right]cos\phi + jA_{21}(n)\left[J_1(u_2) - J_3(u_2)\right]cos2\phi\right\} \tag{2}$$

Manuscript received 9 February 2022; revised 27 October 2022; accepted 12 December 2022. Date of publication 2 February 2023; date of current version 6 March 2023. This work was supported in part by the National Science Foundation (NSF) CAREER Award ECCS-1653915 and in part by the Alabama Established Program to Stimulate Competitive Research (EPSCoR) Graduate Research Scholars Program (Round 16). *(Corresponding author: Maria Pour.)*

The authors are with the Department of Electrical and Computer Engineering, The University of Alabama in Huntsville, Huntsville, AL 35899 USA (e-mail: maria.pour@uah.edu).

Color versions of one or more figures in this communication are available at https://doi.org/10.1109/TAP.2023.3240311.

Digital Object Identifier 10.1109/TAP.2023.3240311

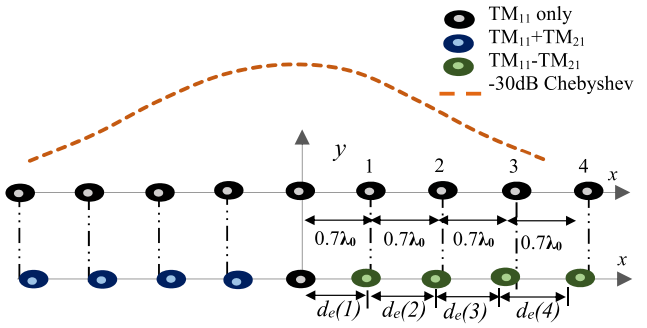

Fig. 2. Structures of the nine-element equally spaced and the proposed E-DPCA array, whose elements are physically placed $0.7\lambda_0$ apart. The optimal tapered element spacing in the E-DPCA array, namely $d_e(1)$–$d_e(4)$, is listed in Table I.

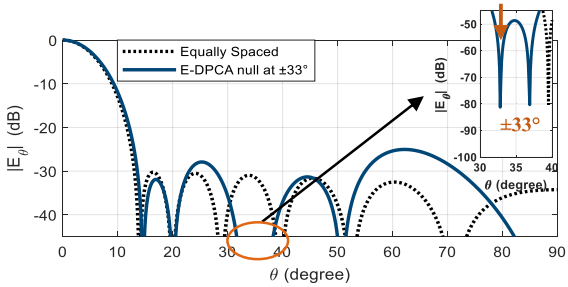

Fig. 3. Radiation patterns of nine-element linear equally spaced (TM_{11} only) array and the proposed E-DPCA array with −30 dB Chebyshev distribution and nulls at ±33°.

where $u_1 = k_0 a_1 \sin\theta$ and $u_2 = k_0 a_2 \sin\theta$; J is the Bessel function of the first kind with associated eigenvalues of 1.841 and 3.054 for the TM_{11} and TM_{21} modes, respectively; a_1 and a_2 are the radii of the circular patches, which are $0.17\lambda_0$ and $0.3\lambda_0$, respectively, λ_0 is the free space wavelength at 10 GHz; $a_p(n)$ is the amplitude excitation coefficient of the n^{th} element of the array and A_{21} is the mode content factor. The physical distance between the adjacent elements and the progressive phase shift are represented by d and β, respectively. Moving the phase center away from the physical center changes the electronic distance between the adjacent elements, which is calculated by

$$d_e(n) = nd + d_{pc}(n) \tag{3}$$

where $d_{pc}(n)$ is the phase center location of the n^{th} antenna element with respect to its physical center. The maximum phase center displacement that can be achieved for this configuration, while keeping the element pattern unchanged, is $d_{pc}(n) = \pm 0.13\lambda_0$ [30], which occurs when $|A_{21}| = 1$.

Using the aforementioned equations, the E-DPCA technique is applied to nine- and 25-element, equally spaced, linear array antennas to electronically change their inter-element spacing by varying the phase center locations to generate steerable nulls without any physical displacement.

A. Nine-Element Linear E-DPCA Array

A nine-element, equally spaced, linear array antenna is constructed using the dual-mode elements placed $0.7\lambda_0$ apart, symmetrically arranged along the x-axis, as illustrated in Fig. 2. Initially, the phase centers of each element are located at their physical centers when only the TM_{11} mode is excited, i.e., $A_{21} = 0\angle 0°$. This is represented by the black "eye" symbols in Fig. 2.

The SLL and minor lobe level of this array configuration are suppressed to −30 dB using a Chebyshev distribution as represented by the orange dashed curve in Fig. 2. To this end, the amplitude excitation coefficients, denoted by a_p in (1), are set per the −30 dB Chebyshev distribution. The corresponding normalized radiation pattern is plotted in Fig. 3 and its peak gain is 16.2 dBi. As the radiation pattern is symmetric about the boresight direction of $\theta = 0°$, only half of the radiation pattern is plotted from $\theta = 0°$ to 90°. The pattern nulls for this array configuration are located at ±14°, ±20°, ±28.8°, ±39.5°, ±52.4°, and ±71.1°, as seen in Fig. 3.

TABLE I

EFFECTIVE DISTANCES BETWEEN ADJACENT ELEMENTS FOR NINE-ELEMENT LINEAR, EQUALLY SPACED, AND E-DPCA ARRAYS WITH −30 DB CHEBYSHEV DISTRIBUTION

	Equally-Spaced (TM_{11})	E-DPCA (TM_{11} +TM_{21}) Null at ±33°	E-DPCA (TM_{11} +TM_{21}) Null at ±24°	E-DPCA (TM_{11} +TM_{21}) Null at ±60°
d_e (1) λ_0	0.7	0.66	0.71	0.75
d_e (2) λ_0	0.7	0.70	0.66	0.70
d_e (3) λ_0	0.7	0.65	0.64	0.73
d_e (4) λ_0	0.7	0.67	0.71	0.69

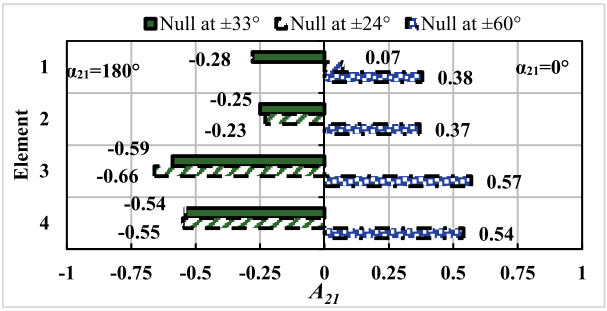

Fig. 4. Optimal A_{21} of the nine-element linear array antenna to steer the nulls to ±24°, ±33°, and ±60°.

To generate nulls at ±33°, without any physical movement, the phase centers of the base elements are symmetrically displaced away from their physical centers to create an electronically aperiodic array configuration. The central element of this E-DPCA array is considered the reference element and its phase center is kept at its physical center by exciting only the TM_{11} mode ($A_{21} = 0\angle 0°$). The elements on either side of the x-axis excite the two modes with the same magnitude but an opposite phase shift. The in- and out-of-phase excitation is pictorially represented by the blue and green "eye" symbols, respectively, in Fig. 2. The magnitudes of the mode content factor in the four elements on either side of the x-axis are $|A_{21}|_{(1)} = 0.28$, $|A_{21}|_{(2)} = 0.25$, $|A_{21}|_{(3)} = 0.59$, and $|A_{21}|_{(4)} = 0.54$, also presented as a bar graph in Fig. 4. This electronically aperiodic configuration now steers the nulls to ±33° per Fig. 3, where the SLLs of the E-DPCA array pattern increase from −30 to −25.6 dB. Such an SLL increase is common in conventional position-only synthesis techniques, as reported in [12], [14], and [18]. The gain of the E-DPCA array reduces from 16.2 to 14.6 dBi due to the excitation of the second mode. The effective distances between the elements in the equally spaced and E-DPCA arrays are compared in Table I. Due to the array symmetry about the x-axis, only the A_{21} values and the resulting element spacings are provided for the right half of the array along the $+x$ axis in Fig. 4 and Table I.

As the direction of the interfering signal can dynamically vary, the pattern nulls need to be steered to different locations without any physical movement. The adaptive null steering capability of the nine-element equally spaced E-DPCA array is further demonstrated by generating two symmetric nulls at ±24° and ±60° without any physical displacement or affecting the main beam. The effective distances between the phase centers of the elements of these E-DPCA

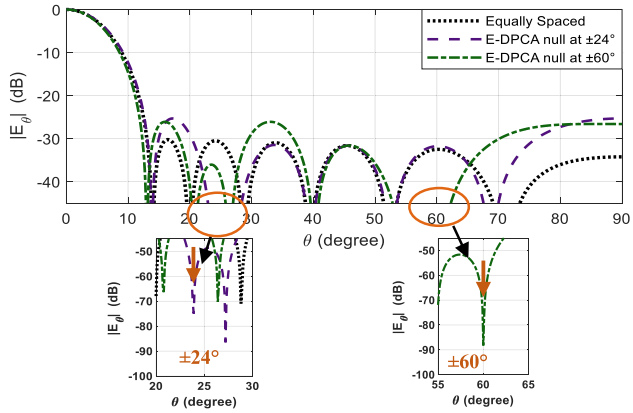

Fig. 5. Radiation patterns of nine-element linear equally spaced (TM_{11} only) and the E-DPCA array with −30 dB Chebyshev distribution and dynamically steered nulls at ±24° and ±60°.

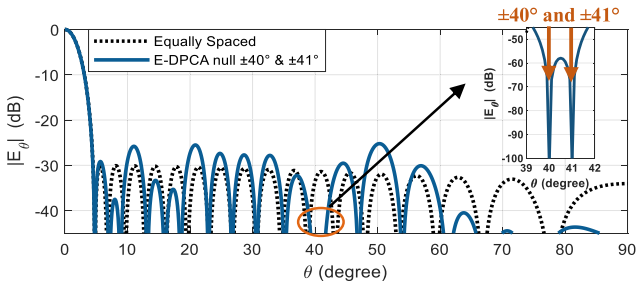

Fig. 6. Radiation patterns of 25-element linear, equally spaced (TM_{11} only) and E-DPCA arrays with −30 dB Chebyshev distribution and two consecutive nulls ±40° and ±41° with a resolution of 1°.

arrays are summarized in Table I and the corresponding mode content factors are given in Fig. 4. The radiation patterns of the E-DPCA arrays that generate the nulls at ±24° and ±60° are overlaid in Fig. 5 and compared with the reference equally spaced array, all of which are excited with the −30 dB Chebyshev distribution. The gain values of the E-DPCA arrays are 14.6 and 14.7 dBi, when the nulls are steered to ±24° and ±60°, respectively.

The A_{21} values required to displace the phase center location of each element in the array to steer the nulls to ±33°, ±24°, and ±60° are determined using the MATLAB built-in genetic algorithm. For the $(2N + 1)$-element linear array, an initial population of 100 chromosomes was chosen such that each chromosome consisted of $2N$ genes. The first N genes contained information on the magnitude of the mode content factor $|A_{21}|$ that controlled the amount of displacements and the remaining N genes contained information on the phase of the mode content factor α_{21} that determined the direction of the displacement. The upper limit of $|A_{21}|$ was set to 1 to maintain broadside element patterns, whereas, α_{21} was set to either 0° or 180°. To evolve toward the optimal values of $|A_{21}|$ and α_{21}, a fitness function (FF) was defined as

$$FF = q_1 \left| ND_t - ND\left(\theta_0\right) \right| + q_2 |SLL_t - SLL| \tag{4}$$

where ND_t is the desired null depth set to −75 dB, $ND\left(\theta_0\right)$ is the depth of the null steered to the desired angle θ_0, SLL_t is the target SLL set to −25 dB, SLL is the sidelobe level of the pattern, and q_1 and q_2 are the respective weights of the FF.

B. 25-Element Linear E-DPCA Array

The null steering capability of the E-DPCA technique is further investigated in a 25-element equally spaced, linear array antenna where the proposed method is employed to create: 1) consecutive nulls with a 1° resolution; 2) nulls with suppressed SLL and minor lobe level; and 3) nulls with scanned main beams.

TABLE II

EFFECTIVE DISTANCES BETWEEN ADJACENT ELEMENTS FOR 25-ELEMENT LINEAR EQUALLY SPACED AND E-DPCA ARRAYS

	Equally-Spaced (TM_{11}) -30dB Chebyshev	E-DPCA Nulls at ±40° and 41°	EDPCA +Thinned Null = ±40.2° SLL =-18.4dB	E-DPCA Main Beam=20° Null=±51.2°
d_e (1) λ_0	0.7	0.72	0.62	0.67
d_e (2) λ_0	0.7	0.73	0.66	0.77
d_e (3) λ_0	0.7	0.71	0.69	0.63
d_e (4) λ_0	0.7	0.67	0.69	0.71
d_e (5) λ_0	0.7	0.62	0.70	0.71
d_e (6) λ_0	0.7	0.72	0.72	0.76
d_e (7) λ_0	0.7	0.70	0.84	0.67
d_e (8) λ_0	0.7	0.79	0.76	0.67
d_e (9) λ_0	0.7	0.61	1.20	0.66
d_e (10) λ_0	0.7	0.73	0.94	0.72
d_e (11) λ_0	0.7	0.80	0.70	0.73
d_e (12) λ_0	0.7	0.66	NA	0.68

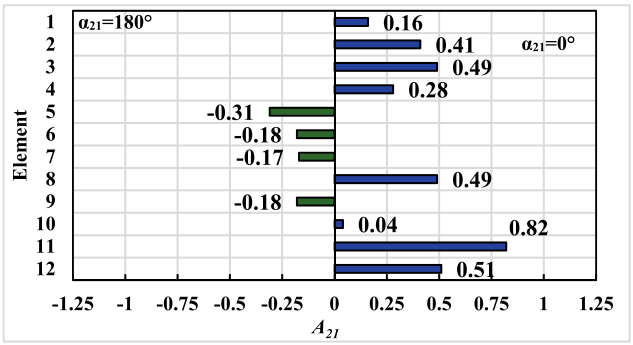

Fig. 7. Optimal mode content factors A_{21} of the 25-element linear array antenna to generate consecutive nulls at ±40° and ±41°.

1) Consecutive Nulls With 1° Resolution: The phase centers of the 25-element equally spaced array antenna were initially kept at their physical centers when only the TM_{11} mode is excited, i.e., $A_{21} = 0\angle 0°$. The associated radiation pattern with a −30 dB Chebyshev distribution, controlled by $a_p(n)$ in (1), has a peak gain of 25 dBi and its normalized radiation pattern is plotted in Fig. 6. To generate two closely spaced nulls, the phase centers of the base elements are electronically displaced away from their physical center by properly exciting the TM_{21} modes in- and out-of-phase with the TM_{11} modes. The resulting electronically aperiodic array generates two nulls with a resolution of 1° between them with a peak gain of 23.6 dBi. The radiation pattern of this E-DPCA array with two consecutive nulls at ±40° and ±41° is overlaid in Fig. 6. The mode content factors required to displace the phase centers at the element level and generate the double-null pattern are summarized in Fig. 7. The effective distances between the phase centers of the adjacent elements in the equally spaced and electronically aperiodic array configurations are compared in Table II.

Additionally, it was observed that the proposed E-DPCA technique can be used to attain this minimum resolution of 1° between consecutive nulls when the minimum number of elements is six.

It is worth noting that the gain of the aforementioned E-DPCA array varies marginally as the location of its consecutive nulls moves toward the main lobe. To demonstrate this, the peak gain for different consecutive nulls with the 1° resolution, including ±10° and ±11°, ±40° and ±41°, and ±80° and ±81°, is plotted in Fig. 8 over the frequency range of 9.8–10.2 GHz. It is observed that the overall

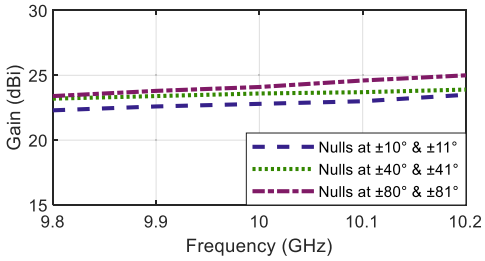

Fig. 8. Gain versus frequency for the 25-element linear E-DPCA array with consecutive nulls at ±10° and ±11°, ±40°and ±41°, and ±80° and ±81°.

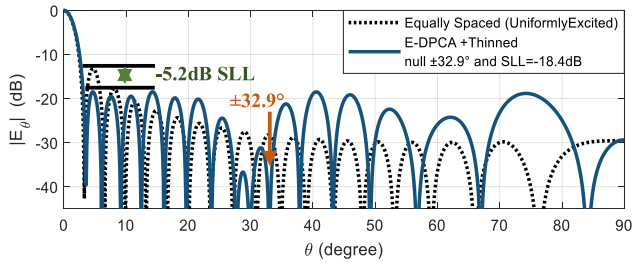

Fig. 9. Radiation patterns of 25-element linear, uniformly excited, equally spaced (TM_{11} only) array and E-DPCA + thinned array with null steered to ±32.9 and SLL below −18.4 dB.

gain of the 25-element E-DPCA array reduces by 1–1.5 dB as the consecutive nulls are moved toward the main lobe. This is mainly due to the larger phase center displacement required to generate the double nulls in the region close to the main lobe. Additionally, as the frequency of operation decreases from 10.2 to 9.8 GHz the overall gain of the array drops by 1.5 dB. Thus, within the ±2% bandwidth of the design frequency of 10 GHz, the E-DPCA array generates consecutive nulls with a resolution as low as 1° without having to increase its overall length or mechanically reposition its base elements.

2) Null Steering With Suppressed SLL and Minor Lobe Level: Thus far, the presented E-DPCA array antennas used the traditional −30 dB Chebyshev distribution to suppress the SLL and minor lobe level while steering the null locations. It has been recently established by Mitha and Pour [30] that the E-DPCA technique when coupled with the array thinning method can reduce the SLL and minor lobe level below −20 dB without any external tapering or physical displacement. In this section, the E-DPCA + thinning technique is used to simultaneously steer the null locations and reduce the SLL and minor lobe level by 5.2 dB. Initially, when only the TM_{11} mode is excited in the 25-element equally spaced linear array, it generates a pattern with the −13.2 dB SLL and the 26.6 dBi peak gain, as shown in Fig. 9. The element spacing of this physically periodic array is electronically tapered by displacing the phase center location of the base elements and turning off the fourth element from the edge on both sides of the array to reduce the SLL and first few minor lobe levels below −18.4 dB and generate symmetric nulls at ±32.9°, without any physical displacement. The resultant E-DPCA array has 22.4 dBi gain and its normalized radiation pattern is plotted in Fig. 9. The optimal mode content factors required for the phase center displacement and the elements needed to be turned off for the array thinning are determined using the MATLAB built-in genetic algorithm. The mode content factor of each element of the thinned EDPCA array and the effective distance between the adjacent elements are summarized in Fig. 10 and Table II, respectively.

3) Simultaneous Beam Scanning and Null Steering: The most popular method of null steering involves controlling the amplitude and phase of the base elements of the array. The phase control, however, limits the arrays' capability to scan the main beam as well as adaptively change the null location. In contrast, the proposed

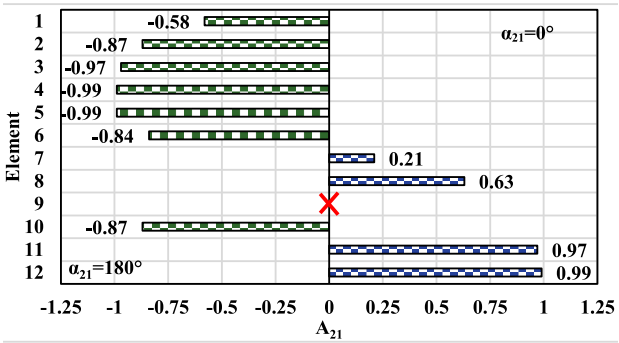

Fig. 10. Optimal mode content factor A_{21} of the 25-element linear array antenna required to steer symmetric nulls to ±32.9° and reduce the SLL and minor lobe level below −18.4 dB.

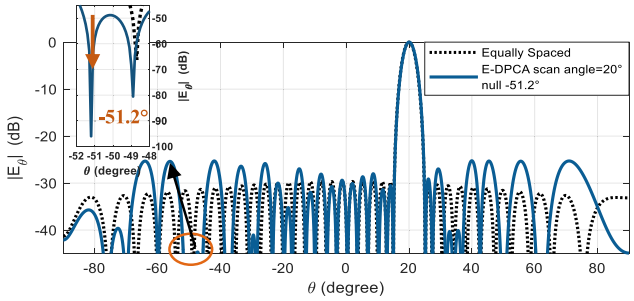

Fig. 11. Radiation patterns of 25-element linear, equally spaced (TM_{11} only) and E-DPCA arrays with −30 dB Chebyshev distribution, main beam scanned to 20° and null steered to −51.2°.

E-DPCA technique does not hinder the array scanning capability, as the phase center displacement is performed within the base element and thus the main beam of the array can be readily scanned in a similar manner as in conventional phased array antennas by applying proper progressive phase shifts at the array level. To scan the main beam away from $\theta = 0°$ the phase term (β) for each element is calculated by

$$\beta(n) = -k_0(nd \pm d_{pc}(n))sin\theta\cos\phi \tag{5}$$

where β is the progressive phase shift of the n^{th} element of the array. As a representative example of the simultaneous beam scanning and null steering capability of the E-DPCA technique, the main beam of the 25-element equally spaced array antenna is scanned to $\theta = 20°$ while simultaneously steering the null to −51.2°. Initially, the main beam of the equally spaced array is scanned to 20° at the array level while maintaining the phase centers at the physical centers and suppressing the SLL and minor lobe level using a −30 dB Chebyshev distribution, as presented in Fig. 11. The peak gain of this scanned pattern is 24.8 dBi. To simultaneously steer the null locations and scan the main beam, the phase center locations of the 25-element equally spaced array are electronically displaced away from their physical centers at the element level, creating an electronically aperiodic configuration. This E-DPCA array now generates a null at −51.2° while scanning the main beam to $\theta = 20°$ as shown in Fig. 11, without any physical displacement. The overall gain of the E-DPCA array reduces to 23.4 dBi. The required mode content factor to displace the phase center in each element is summarized in Fig. 12 and the resultant distances between the adjacent elements are listed in Table II.

From the above analyses, it can be concluded that the E-DPCA technique may be used in equally spaced array antennas to steer not just a single null but also consecutive nulls with a minimum resolution of 1° between them. The proposed technique can be further applied to simultaneously steer the nulls and scan the main beam. Additionally, the E-DPCA technique can be combined with the array thinning to

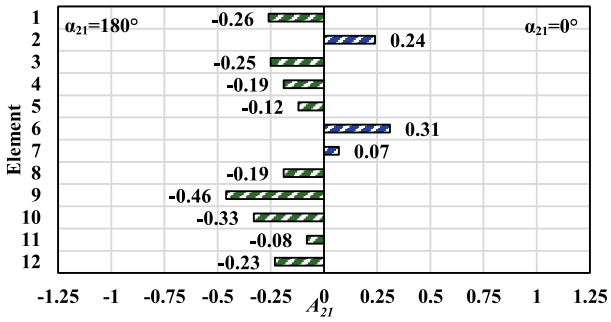

Fig. 12. Optimal mode content factor A_{21} of the 25-element linear array antenna required to steer the null to $-51.2°$ while scanning the main beam to 20°.

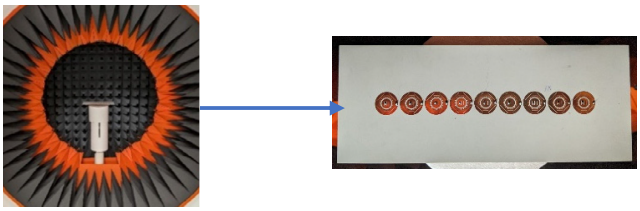

Fig. 13. Photograph of the fabricated nine-element, dual-mode linear array antenna under test in an anechoic chamber.

achieve dynamic null steering and reduce the side and minor lobe without physically moving the base elements, while maintaining the overall array size.

III. Simulated and Measured Results of Nine-Element Linear Array Antenna

The null steering capability of the nine-element linear array antenna discussed in Section II-A is further validated through its full-wave analysis using a finite-element-based electromagnetic solver ANSYS HFSS [31]. The full-wave analysis takes into consideration the mutual coupling and edge and probe effects that may alter the overall radiation pattern. To ease the fabrication and assembly, the nine-element linear E-DPCA array is designed using the single-layer dual-mode antenna element [29], [30], [32] that excites the TM_{11} and TM_{21} modes at the frequency of 10 GHz. Based on the full-wave analysis, the single-layer nine-element array antenna was fabricated and tested in the spherical near-field anechoic chamber at the University of Alabama in Huntsville. A photograph of the antenna under test is shown in Fig. 13.

The measured and simulated active and passive scattering parameters of this nine-element linear array were reported in [30] and thus are not repeated here for brevity. Per [30], the highest mutual coupling, which occurred between the adjacent elements, was about -13 dB. To compensate for the mutual coupling, as well as the probes' asymmetry and the edge effects, the required mode content factors need to be slightly adjusted from those obtained by the analytical cavity model to generate deep nulls using the E-DPCA technique.

The total radiation pattern of the nine-element linear array antenna, i.e., E_θ^{Total} in (1), is computed by measuring the active radiation patterns of the central and edge elements, according to [33] and [34] as these elements contain the majority of information about the mutual coupling and edge effects. As per Section II-A, initially, when only the TM_{11} modes are excited with the -30 dB Chebyshev distribution, the nine-element equally spaced array antenna generates a pattern with the nulls at $\pm14°$, $\pm20.2°$, $\pm29°$, $\pm39.1°$, $\pm51°$, and $\pm66°$, as plotted in Fig. 14(a). The phase centers of each element of this equally spaced array are located at their physical centers as the TM_{21} modes are turned off for this configuration. As a representative

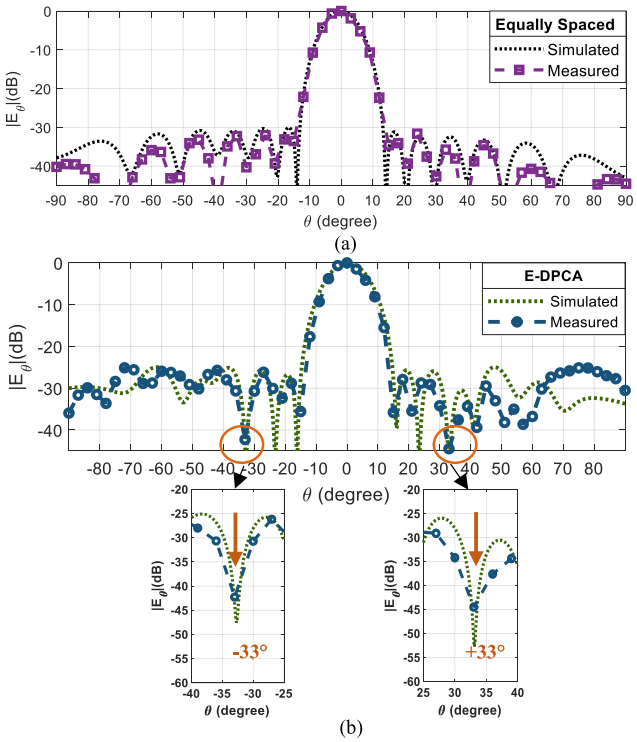

Fig. 14. Measured and simulated radiation patterns of the nine-element. (a) Equally spaced (TM_{11} only) and (b) proposed E-DPCA array with -30 dB Chebyshev distribution and nulls steered to $\pm33°$.

TABLE III
Effective Distances Between Adjacent Elements for Nine-Element Equally Spaced and E-DPCA Array With -30 dB Chebyshev Distribution

	Equally-Spaced (TM_{11})	E-DPCA (TM_{11} +TM_{21}) Null at ±33°
d_e (1) λ_0	0.7	0.66
d_e (2) λ_0	0.7	0.69
d_e (3) λ_0	0.7	0.73
d_e (4) λ_0	0.7	0.73
d_e (5) λ_0	0.7	0.76
d_e (6) λ_0	0.7	0.71
d_e (7) λ_0	0.7	0.71
d_e (8) λ_0	0.7	0.67

example of the null steering capability of this nine-element E-DPCA array, symmetric nulls are introduced at $\pm33°$ without physically moving any of the elements of the array. The adjusted mode content factors of each element of the E-DPCA array and the effective distance between the adjacent elements are summarized in Fig. 15 and Table III, respectively, compensating for the mutual coupling, probes' asymmetry, and edge effects. The simulated and measured radiation patterns for the equally spaced, single-mode array, and the proposed E-DPCA array compared in Fig. 14(a) and (b), respectively, are in good agreement with each other and follow a similar trend. Small discrepancies are observed between the simulated and measured radiation patterns on account of the mutual coupling and edge effects. Despite these small disparities, both the measured and simulated E-DPCA arrays generate a steep null at $\pm33°$ with a respectable null depth of -45 dB. The simulated and measured gain values of the equally spaced arrays with the -30 dB Chebyshev taper are 16.15 and 16 dBi, respectively, whereas, those of the E-DPCA array are 14.28 and 14.1 dBi, respectively. Additionally, both the simulated and measured results show an increase in the SLL and minor lobe

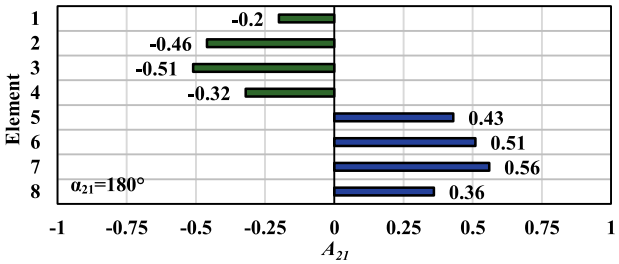

Fig. 15. Optimal A_{21} of the nine-element linear array antenna to steer the nulls to $\pm 24°$.

level from -30 to -25 dB, which is similar to the nine-element linear array antenna analyzed in Section II-A.

The presented measured and simulated results successfully validate the proposed theory that the EDPCA technique can be utilized to adaptively steer the null location of N-element linear array antennas by electronically transforming them into aperiodic structures without any physical movement, while preserving the original array length.

IV. Conclusion

A novel method of dynamically steering the null locations in equally spaced linear array antennas using the E-DPCA technique has been introduced for the first time in this communication. The potential of the proposed technique was first examined in a nine-element linear array antenna, wherein symmetric nulls were generated without any physical displacement. The versatility of the E-DPCA technique was further explored in a 25-element linear array by: 1) generating consecutive nulls with a minimum resolution of 1° between them and 2) simultaneously steering the nulls and scanning the main beam. As a proof of concept, the nine-element E-DPCA array was full-wave analyzed, fabricated, and tested in an anechoic chamber. The measured and simulated results were in good agreement with each other, which further validated the practical implementation of the proposed E-DPCA technique in adaptively steering the null locations without physically moving the elements or increasing the overall array size.

References

[1] C. A. Balanis, *Antenna Theory: Analysis and Design*, 4th ed. Hoboken, NJ, USA: Wiley, 2016.

[2] C. Baird and G. Rassweiler, "Adaptive sidelobe nulling using digitally controlled phase-shifters," *IEEE Trans. Antennas Propag.*, vol. AP-24, no. 5, pp. 638–649, Sep. 1976.

[3] H. Steyskal, "Simple method for pattern nulling by phase perturbation," *IEEE Trans. Antennas Propag.*, vol. AP-31, no. 1, pp. 163–166, Jan. 1983.

[4] R. Vescovo, "Null synthesis by phase control for antenna arrays," *Electron. Lett.*, vol. 36, no. 33, pp. 198–199, 2000.

[5] R. A. Shore, "Nulling a symmetric pattern location with phase-only weight control," *IEEE Trans. Antennas Propag.*, vol.AP- 32, no. 5, pp. 530–533, May 1984.

[6] T. Vu, "Simultaneous nulling in sum and difference patterns by amplitude control," *IEEE Trans. Antennas Propag.*, vol. AP-34, no. 2, pp. 214–218, Feb. 1986.

[7] T. B. Vu, "Method of null steering without using phase shifters," *IEE Proc. H (Microw., Opt. Antennas)*, vol. 131, pp. 242–246, Aug. 1984.

[8] R. L. Haupt, "Simultaneous nulling in the sum and difference patterns of a monopulse antenna," *IEEE Trans. Antennas Propag.*, vol. AP-32, no. 5, pp. 486–493, May 1984.

[9] H. Steyskal, R. Shore, and R. Haupt, "Methods for null control and their effects on the radiation pattern," *IEEE Trans. Antennas Propag.*, vol. AP-34, no. 3, pp. 404–409, Mar. 1986.

[10] S. Applebaum, "Adaptive arrays," *IEEE Trans. Antennas Propag.*, vol. AP-24, no. 5, pp. 585–598, Sep. 1976.

[11] R. L. Haupt, "Null synthesis with phase and amplitude controls at the subarray outputs," *IEEE Trans. Antennas Propag.*, vol. AP-33, no. 5, pp. 505–509, May 1985.

[12] T. H. Ismail and M. A. Dawoud, "Null steering in phased arrays by controlling the element positions," *IEEE Trans. Antennas Propag.*, vol. 39, no. 11, pp. 1561–1566, Nov. 1991.

[13] M. M. Dawoud and T. H. Ismail, "Experimental verification of null steering by element position perturbations," *IEEE Trans. Antennas Propag.*, vol. 40, no. 11, pp. 1431–1434, Nov. 1992.

[14] J. A. Hejres, "Null steering in phased arrays by controlling the positions of selected elements," *IEEE Trans. Antennas Propag.*, vol. 52, no. 11, pp. 2891–2895, Nov. 2004.

[15] R. L. Haupt, "Phase-only adaptive nulling with a genetic algorithm," *IEEE Trans. Antennas Propag.*, vol. 45, no. 6, pp. 1009–1015, Jun. 1997.

[16] K. Guney and M. Onay, "Amplitude-only pattern nulling of linear antenna arrays with the use of bees algorithm," *Prog. Electromagn. Res.*, vol. 70, pp. 21–36, 2007.

[17] M. A.-A. Mangoud and H. M. Elragal, "Antenna array pattern synthesis and wide null control using ENHANCED particle swarm optimization," *Prog. Electromagn. Res. B*, vol. 17, pp. 1–14, 2009.

[18] A. Tennant, M. M. Dawoud, and A. P. Anderson, "Array pattern nulling by element position perturbations using a genetic algorithm," *Electron. Lett.*, vol. 30, no. 3, pp. 174–176, Feb. 1994.

[19] T. H. Ismail and Z. M. Hamici, "Array pattern synthesis using digital phase control by quantized particle swarm optimization," *IEEE Trans. Antennas Propag.*, vol. 58, no. 6, pp. 2142–2145, Jun. 2010.

[20] M. M. Khodier and C. G. Christodoulou, "Linear array geometry synthesis with minimum sidelobe level and null control using particle swarm optimization," *IEEE Trans. Antennas Propag.*, vol. 53, no. 8, pp. 2674–2679, Aug. 2005.

[21] S. K. Goudos, V. Moysiadou, T. Samaras, K. Siakavara, and J. N. Sahalos, "Application of a comprehensive learning particle swarm optimizer to unequally spaced linear array synthesis with sidelobe level suppression and null control," *IEEE Antennas Wireless Propag. Lett.*, vol. 9, pp. 125–129, 2010.

[22] M. I. Skolnik, *Radar Handbook*. New York, NY, USA: McGraw-Hill, 1990.

[23] L. Shafai, S. K. Sharma, B. Balaji, A. Damini, and G. Haslam, "Multiple phase center performance of reflector antennas using a dual mode horn," *IEEE Trans. Antennas Propag.*, vol. 54, no. 11, pp. 3407–3417, Nov. 2006.

[24] Z. A. Pour and L. Shafai, "Investigation of virtual array antennas with adaptive element locations and polarization using parabolic reflector antennas," *IEEE Trans. Antennas Propag.*, vol. 61, no. 2, pp. 688–699, Feb. 2013.

[25] Z. A. Pour and L. Shafai, "Improved cross-polarization performance of a multi-phase-center parabolic reflector antenna," *IEEE Antennas Wireless Propag. Lett.*, vol. 13, pp. 540–543, 2014.

[26] Z. A. Pour, "Control of phase center and polarization in circular microstrip antennas," M.S. thesis, Dept. Elect. Eng., Univ. Manitoba, Winnipeg, MB, Canada, Jul. 2006.

[27] Z. A. Pour and L. Shafai, "Adaptive aperture antennas with adjustable phase centre locations," in *Proc. IEEE Int. Workshop Antenna Technol. (iWAT)*, Tucson, AZ, USA, Mar. 2012, pp. 355–357.

[28] Z. A. Pour, L. Shafai, and A. M. Mehrabani, "Virtual array antenna with displaced phase centers for GMTI applications," in *Proc. IEEE RadarCon (RADAR)*, Kansas City, MO, USA, May 2011, pp. 830–834.

[29] T. Mitha and M. Pour, "Principles of adaptive element spacing in linear array antennas," *Sci. Rep.*, vol. 11, no. 1, p. 5584, 2021.

[30] T. H. Mitha and M. Pour, "Sidelobe reductions in linear array antennas using electronically displaced phase center antenna technique," *IEEE Trans. Antennas Propag.*, vol. 70, no. 6, pp. 4369–4378, Jun. 2022, doi: 10.1109/TAP.2021.3138499.

[31] *High Frequency Structure Simulator (HFSS 20.0)*, ANSYS, Canonsburg, PA, USA, 2020.

[32] Z. Iqbal, T. Mitha, and M. Pour, "A self-nulling single-layer dual-mode microstrip patch antenna for grating lobe reduction," *IEEE Antennas Wireless Propag. Lett.*, vol. 19, no. 9, pp. 1506–1510, Sep. 2020.

[33] D. M. Pozar, "The active element pattern," *IEEE Trans. Antennas Propag.*, vol. 42, no. 8, pp. 1176–1178, Sep. 1994.

[34] D. F. Kelley and W. L. Stutzman, "Array antenna pattern modeling methods that include mutual coupling effects," *IEEE Trans. Antennas Propag.*, vol. 41, no. 12, pp. 1625–1632, Dec. 1993.